

Article

Efficient Conversion of Ethanol to Hydrogen in a Hybrid Plasma-Catalytic Reactor

Bogdan Ulejczyk ^{1,*}, Paweł Józwiak ², Łukasz Nogal ³, Michał Młotek ¹ and Krzysztof Krawczyk ¹

¹ Faculty of Chemistry, Warsaw University of Technology, Noakowskiego 3, 00-664 Warsaw, Poland; michal.mlotek@pw.edu.pl (M.M.); kraw@ch.pw.edu.pl (K.K.)

² Faculty of Advanced Technologies and Chemistry, Military University of Technology, Gen. S. Kaliskiego 2, 00-908 Warsaw, Poland; pjozwiak@wat.edu.pl

³ Faculty of Electrical Engineering, Warsaw University of Technology, Pl. Politechniki 1, 00-661 Warsaw, Poland; lukasz.nogal@ien.pw.edu.pl

* Correspondence: bulejczyk@ch.pw.edu.pl

Abstract: The present work describes highly efficient hydrogen production from ethanol in a plasma-catalytic reactor depending on the discharge power and catalyst bed temperature. Hydrogen production increased as the power increased from 15 to 25 W. A further power increase to 35 W did not increase hydrogen production. The catalyst was already active at a temperature of 250 °C, and its activity increased with increasing temperature to 450 °C. The further temperature increase did not increase the activity of the cobalt catalyst. The most important advantage of using the catalyst was the increased ethanol conversion to CO₂ instead of CO production. As a result, the hydrogen yield was very high and reached 4.1 mol(H₂)/mol(C₂H₅OH). This result was obtained with a stoichiometric molar ratio of water to ethanol of 3.



Citation: Ulejczyk, B.; Józwiak, P.; Nogal, Ł.; Młotek, M.; Krawczyk, K. Efficient Conversion of Ethanol to Hydrogen in a Hybrid Plasma-Catalytic Reactor. *Energies* **2022**, *15*, 3050. <https://doi.org/10.3390/en15093050>

Academic Editors: Grzegorz Wałowski, Adam Smoliński and Javier Fermoso

Received: 18 March 2022

Accepted: 20 April 2022

Published: 21 April 2022

Publisher's Note: MDPI stays neutral with regard to jurisdictional claims in published maps and institutional affiliations.



Copyright: © 2022 by the authors. Licensee MDPI, Basel, Switzerland. This article is an open access article distributed under the terms and conditions of the Creative Commons Attribution (CC BY) license (<https://creativecommons.org/licenses/by/4.0/>).

Keywords: ethanol; hydrogen; reforming

1. Introduction

Primary energy consumption in 2020 was 556.83 EJ. Currently, the main sources of energy are crude oil (31%), coal (27%), and natural gas (25%). Due to the use of these fuels, CO₂ emissions exceeded 32 billion tons. Other energy sources not emitting CO₂ are nuclear energy (4%), hydropower (7%), and renewable sources (6%). Their share in electricity production is more significant and amounts to 10, 16, and 12%, respectively, because, for example, crude oil is mainly used in transport. Renewable energy is developing rapidly, annually, by ~13%. Currently, wind energy is of the most significant importance, but solar energy production is growing the fastest [1]. A substantial barrier to developing these two renewable energies is their dependence on weather conditions.

Hydrogen energy is not yet profitable, and an effective method of obtaining hydrogen from renewable resources, e.g., water, biogas, bio-alcohols, has to be developed. Research and development work on technologies for hydrogen production from these renewable resources are carried out in many research centers. Traditional water electrolysis technology is not energy efficient. However, new and more efficient electrolyzers are constantly being constructed. Sarno and Ponticorvo [2] reported that in an electrolyzer with a cathode coated with a nanocatalyst (RuS₂ and MoS₂), the cost of hydrogen production was 3.8 kWh/Nm³. Research on biogas and bio-alcohol conversion focuses on developing catalysts, plasma and plasma-catalytic reactors enabling hydrogen production from these raw materials.

Biogas contains 30 to 70% CH₄, which is the source of H₂. The second component of biogas is CO₂, the concentration of which ranges from 25 to 50% [3]. The presence of CO₂ in the raw material inhibits hydrogen production from biogas (CH₄ + 2H₂O ⇌ 4H₂ + CO₂) and results in small efficiency. Lachen et al. [4] reported that hydrogen production from

biogas was from 0.4 to 0.8 mol(H₂)/mol(CH₄). In addition, researchers observed that H₂ production decreased with increasing CO₂ content in the catalytic process [4].

Bio-alcohols are liquids and, after distillation, do not contain impurities that adversely affect the process of hydrogen production. Therefore, the yield of hydrogen production from bio-alcohols can be higher than from biogas. Tahir et al. [5] synthesized a cobalt catalyst on which the highest hydrogen yield achieved was 3 mol(H₂)/mol(C₂H₅OH). Mosińska et al. [6] synthesized a nickel catalyst on which the highest hydrogen yield achieved was 2.1 mol(H₂)/mol(CH₃OH). The research on and comparisons of catalytic processes are very complex because different catalysts are active in the steam reforming process of methanol and ethanol. Konsalokakis et al. [7] reported that cobalt showed higher activity than nickel in the steam reforming of ethanol, whereas Ma et al. [8] reported that nickel showed higher activity than cobalt in the steam reforming of methanol.

Tatarova et al. [9] reported that in the microwave discharge, maximal hydrogen yield was 1.72 mol(H₂)/mol(CH₃OH) or 3.01 mol(H₂)/mol(C₂H₅OH), respectively. Our previous studies on the spark discharge showed that more hydrogen could be obtained from ethanol than from methanol [10–12]. In contrast, Burlica et al. [13] reported that in the gliding discharge, the process of hydrogen production from methanol was higher than that from ethanol. Our previous research also indicated that a discharge type significantly affects hydrogen production. The hydrogen yield was 1.12 mol(H₂)/mol(C₂H₅OH) [14] in a dielectric barrier discharge, whereas in a spark discharge, the hydrogen yield was higher and reached 2.01 mol(H₂)/mol(C₂H₅OH) [12]. A higher temperature is achieved in a spark discharge than in a barrier discharge. Therefore, a spark discharge is more effective than a barrier discharge. The advantage of a spark discharge over sliding and microwave discharges is the possibility of working without additional gases, allowing the process to generate discharges. A significant advantage of a spark discharge is the reliable and simple design of the reactor.

One of the methods of increasing the efficiency of converting alcohol into hydrogen is using hybrid plasma-catalytic systems. The use of hybrid plasma-catalytic techniques made it possible to achieve higher hydrogen production than in plasma reactors [15–19]. Positive effects of using plasma-catalytic reactors were also observed in hydrogen production from biogas [20–22].

This work presents a plasma-catalytic reactor with a cobalt catalyst combined with plasma generated by a spark discharge. A spark discharge allows higher ethanol conversion, while a cobalt catalyst enables increased ethanol conversion to hydrogen and carbon dioxide [23]. Instead of a supported catalyst, an innovative metal catalyst was used because it does not reduce the amount of metal on the surface and is resistant to sintering. Sintering and reduction of the metal content on the surface of supported catalysts are important factors in catalyst deactivation [7,24,25]. These processes are irreversible and mean that spent catalysts must be disposed of. In the case of an unsupported metal catalyst, these two disadvantageous phenomena do not occur. The cobalt catalyst enables the efficient production of hydrogen from ethanol. Ethanol allows more hydrogen to be produced per alcohol consumed compared to methanol. Additionally, ethanol is cheaper than methanol because it is easier to produce from biomass. The advantage of a spark discharge is the presence of electrons of such high energy as to cause dissociation of chemical bonds in water and ethanol molecules. Maintaining the appropriate distance between the electrodes and the catalyst prevents the electrodes from shorting and enables the long-term operation of the plasma-catalytic reactor.

2. Materials and Methods

The methods and apparatus used in the research were described in detail in our previous study of Ulejczyk et al. [12,19]. In addition to the previously used SEM and EDS methods to characterize the catalyst, this work also examined the catalyst using X-ray diffraction (XRD) and temperature-programmed oxidation (TPO). The XRD was performed with a Rigaku Ultima IV diffractometer with a Co lamp using a 40 kV voltage

and a 40 mA current. The TPO experiment was performed with a TA-Instruments SDT Q600 thermogravimetric analyzer at 100 mL/min airflow and a temperature rise rate of 10 °C/min.

Herein, the conditions of the experiments are presented in Table 1. The volume of the plasma zone was ~90 mm³. The catalyst with a mass of 1 g and a specific surface area of 1.75 m²/g was placed in the reactor. The detailed procedure of the catalyst preparation can be found elsewhere [23]. The distance between the ends of the electrodes and the catalyst's surface was 1 cm.

Table 1. Parameters of experiments.

Ethanol feed flow	0.25 mol/h
Water feed flow	0.75 mol/h
Discharge power	15–35 W
Catalyst mass	1 g
Temperature of the catalyst bed	250–600 °C

Distilled water obtained in the DE20plus distiller (Polna S.A., Przemyśl, Poland) and 96% ethanol p.a. (POCh S.A., Gliwice, Poland) were used in the research.

The plasma-catalytic reactor's performance was based on ethanol conversion, hydrogen yield, and production of hydrogen, carbon monoxide, carbon dioxide, methane, acetylene, and ethylene. Each experiment was run for 2 h, and an average of three measurements was used for the calculation. The first sample for chromatographic analysis was taken after 30 min and then every 45 min. The catalyst stability studies were conducted for 5 days. Each day the process was conducted for 5 h.

Equations (1)–(8) were used for the calculations:

$$\text{H}_2 \text{ production (L/h)} = \text{gas flow under standard conditions} \times \text{H}_2 \text{ concentration} \quad (1)$$

$$\text{CO production (L/h)} = \text{gas flow under standard conditions} \times \text{CO concentration} \quad (2)$$

$$\text{CO}_2 \text{ production (L/h)} = \text{gas flow under standard conditions} \times \text{CO}_2 \text{ concentration} \quad (3)$$

$$\text{CH}_4 \text{ production (L/h)} = \text{gas flow under standard conditions} \times \text{CH}_4 \text{ concentration} \quad (4)$$

$$\text{C}_2\text{H}_2 \text{ production (L/h)} = \text{gas flow under standard conditions} \times \text{C}_2\text{H}_2 \text{ concentration} \quad (5)$$

$$\text{C}_2\text{H}_4 \text{ production (L/h)} = \text{gas flow under standard conditions} \times \text{C}_2\text{H}_4 \text{ concentration} \quad (6)$$

$$\text{C}_2\text{H}_5\text{OH conversion (\%)} = \text{moles of C}_2\text{H}_5\text{OH converted} / \text{moles of C}_2\text{H}_5\text{OH feed} \times 100 \quad (7)$$

$$\text{H}_2 \text{ yield (mol}_{\text{hydrogen}}/\text{mol}_{\text{ethanol}}) = \text{moles of H}_2 \text{ produced} / \text{moles of C}_2\text{H}_5\text{OH converted} \quad (8)$$

3. Results

Figures 1 and 2 show the effect of the discharge power and the catalyst bed temperature on the ethanol conversion and hydrogen production. Increasing the discharge power from 15 to 25 W caused a significant increase in both ethanol conversion and hydrogen production. In contrast, the hydrogen production and ethanol conversion at 25 and 35 W power were almost the same when the catalyst bed temperature was the same. The analogous phenomenon occurred in a spark discharge without a catalyst. Increasing the discharge power resulted in slight increases in hydrogen production and conversion, which increased energy consumption in the hydrogen production process [12]. Our earlier publication [23] presents the results of hydrogen production on the cobalt catalyst used in this study. The cobalt catalyst was active from the temperature of 350 °C. The catalyst was active at a lower temperature in a hybrid plasma-catalytic system. Already at a temperature of 250 °C, an increase in hydrogen production and ethanol conversion was observed compared to the plasma-catalytic reactor in which the catalyst was not heated. The temperature range over which the catalyst achieves very high activity was also widened.

In the plasma-catalytic reactor at temperatures from 450 to 600 °C, hydrogen production was very high. On the other hand, the hydrogen production in the catalytic reactor was very high in the temperature range of 500–600 °C.

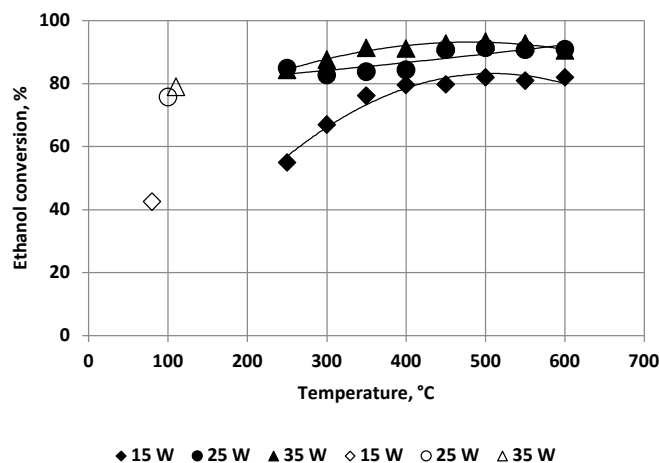


Figure 1. The ethanol conversion (markers with background relate to a process in which the catalyst was not heated).

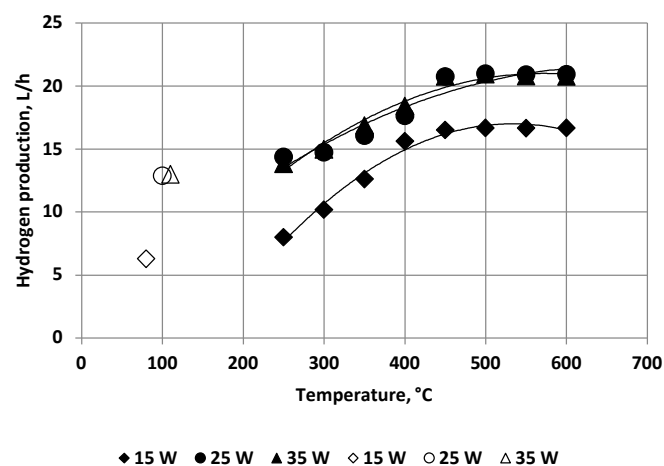
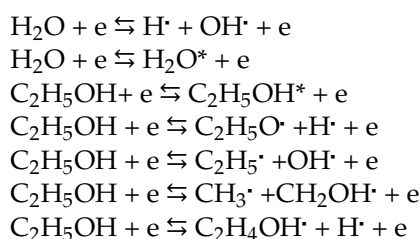


Figure 2. The hydrogen production (markers with background relate to a process in which the catalyst was not heated).

It can be assumed that the change in the catalyst activity range results from a change in the composition of the gas introduced into the catalyst bed. Some ethanol and water reacted to form radicals and stable products in the plasma. The reactions initiating the chemical process in a spark discharge proceed with the participation of electrons and lead to the formation of radicals or excited molecules:



Next, the reactions leading to various stable products, e.g., H_2 , CO , CO_2 , CH_2O , CH_4 , C_2H_4 , C_2H_2 , and coke, occur. The reactions in the plasma have been described in detail in our previous publications [12,19,26]. The reactions with the radicals are very fast because the radicals are very reactive. Therefore, only unreacted substrates and stable products

reached the catalyst bed because the distance between the electrodes and the catalyst was 10 mm, and the radicals disappeared after traveling ~1 mm [27].

However, the passage through the plasma zone increased the internal energy of the molecules because collisions with electrons of energy lower than that necessary for the dissociation of chemical bonds increased the internal energy (Figure 3). The spark discharge was also a source of photons, which also raised the internal energy of the molecules. Moreover, the increase in internal energy caused the activation energy of the excited molecules with the catalyst and each other to decrease. As a result, the reactions could occur at a lower temperature, and the chemical process was very efficient. Lowering the temperature by 50 °C resulted in a reduction in energy consumption. For ethanol (0.25 mol/h) and water (0.75 mol/h) streams, the savings were 1.54 and 1.43 kJ/h, respectively.

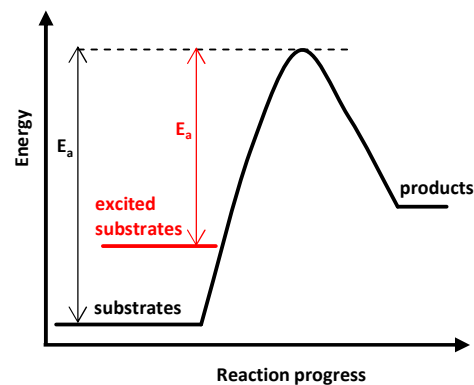


Figure 3. The effect of molecule excitation on the activation energy (E_a).

It is noteworthy that the effect of the catalyst on hydrogen production was more significant than on ethanol conversion due to the increase in CO_2 production (Figure 4).

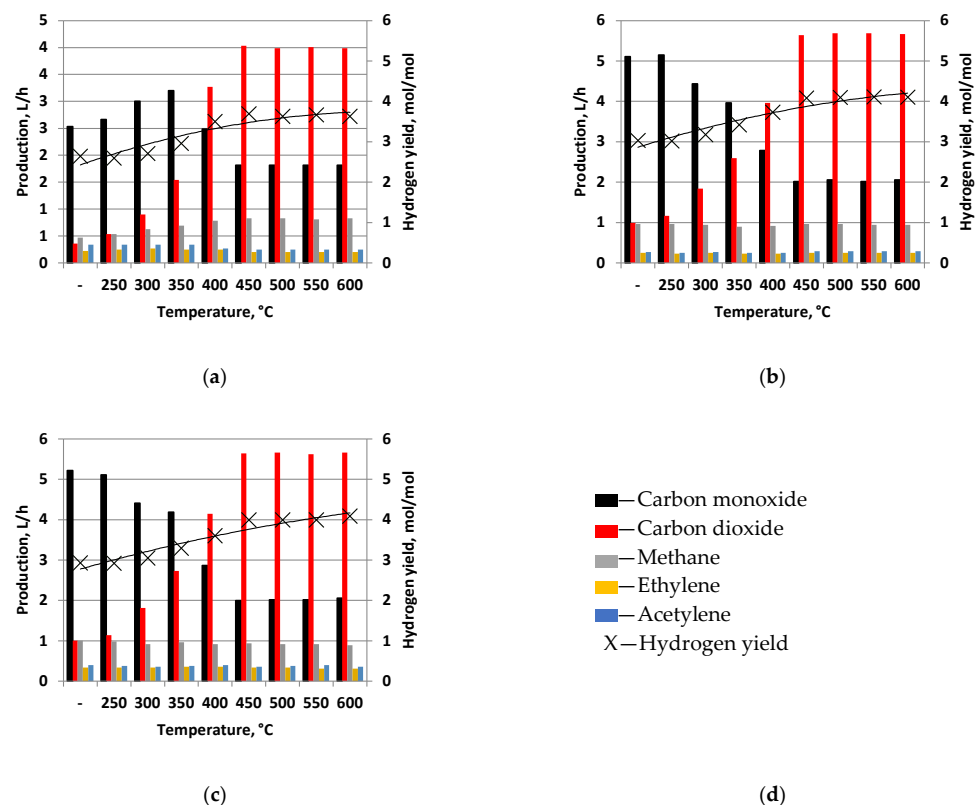


Figure 4. The influence of the catalyst temperature on various compounds and hydrogen yield. Discharge power: (a) 15 W; (b) 25 W; (c) 35 W. (d) Legend for charts.

Even stable substrates can be dissociated with high efficiency in plasma, and chemical reactions involving them can be initiated. On the other hand, collisions with electrons that initiate chemical reactions in plasma are not very selective, and plasma processes are usually non-selective. In contrast, catalytic processes are selective, but they are sensitive to the temperature and purity of the substrates. There was a negligible amount of ethylene and acetylene in the products obtained on the cobalt catalyst [23]. On the other hand, in the spark discharge, the production of these hydrocarbons was many times greater [10,12].

The introduction of the catalyst behind the plasma zone did not limit the conversion of ethanol to ethylene and acetylene. The production of hydrocarbons changed with the change in discharge power. On the other hand, the catalyst bed temperature slightly influenced the production of hydrocarbons. The effect was visible only at the lowest discharge power, i.e., 15 W. For this power, CH₄ production increased from 0.47 to 0.83 L/h with the temperature increase to 450 °C and remained at this level despite further temperature increases, while the production of C₂H₂ decreased from 0.34 to 0.25 L/h as the temperature increased to 450 °C and remained at this level despite further temperature increases. C₂H₄ production reached the maximum value (0.27 L/h) at the catalyst bed temperature of 300 °C, and from 450 °C, the production of C₂H₄ did not change and amounted to 0.2 L/h. Hydrogen production from ethanol at a discharge power of 15 W was already relatively high. On the other hand, the production of hydrogen from methanol in the plasma-catalytic reactor at 15 W was small [19]. These processes differed in the catalyst, but ethanol is also a more reactive chemical than methanol. The greater reactivity of ethanol was confirmed in reactions with the hydroxyl radical [28] and atomic oxygen [29].

For the powers of 25 W and 35 W, CH₄, C₂H₂, and C₂H₄ production did not depend on the catalyst bed temperature. This result indicated that the catalyst was practically inactive in the hydrocarbon and steam reactions. On the other hand, the increase in ethanol conversion and hydrogen and carbon dioxide production and the decrease in carbon monoxide production indicated that the cobalt catalyst was active in the ethanol steam reforming (C₂H₅OH + H₂O ⇌ 4H₂ + CO) and water–gas shift (CO + H₂O ⇌ H₂ + CO₂) reactions. The change in ethanol conversion was relatively small as most of the ethanol reacted in the plasma. In contrast, the increase in CO₂ production and the reduction in CO production were significant. The high activity of cobalt catalysts in water–gas shift reactions was also observed by Baraj et al. [30].

The changes in hydrocarbon production observed with the discharge power of 15 W resulted from the ethanol reaction on the catalyst. The effect of changes on the catalyst was observable because the change in ethanol conversion was almost two-fold. In the reactor where the catalyst was not heated and inactive, the ethanol conversion was 43%. When the catalytic bed temperature was 250 °C, the ethanol conversion was 55% and increased to 80% as the catalyst bed temperature increased to 450 °C. On the other hand, when the discharge power was 25 and 35 W, the ethanol conversion increased to a lesser extent, and no changes in the production of hydrocarbons were observed. The ethanol conversion was 76 and 79%, respectively, in the reactor with an unheated catalyst bed. Heating the catalyst bed to 250 °C increased the ethanol conversion to 85 and 84%, respectively. Increasing the catalyst bed temperature to 450 °C caused an increase in the ethanol conversion to 91 and 93%, respectively.

The most important advantage of using the plasma-catalytic reactor was the possibility of achieving high selectivity of CO₂ production. CO was the main carbon-containing product [10,27,31–36] in the plasma reactors. CO₂ was produced many times less than CO in these reactors. In contrast, the cobalt catalyst favored the water–gas shift reaction. With the catalyst bed temperature increase, the CO₂ production increased, and the CO production decreased. It is a positive phenomenon because hydrogen is produced in the water–gas shift reaction. The more CO that reacts with the steam, the greater the hydrogen yield. The highest hydrogen yield was 4.1 mol(H₂)/mol(C₂H₅OH), and it was 68.5% of the theoretical yield of hydrogen production. The high value of hydrogen yield was achieved with a water/ethanol molar ratio of 3. Increasing the water/ethanol molar ratio allows

for greater hydrogen production efficiency but increases the process's energy costs [26]. Using a stoichiometric molar ratio of the substrates means less energy must be spent to heat and evaporate them. Our calculations presented in the earlier publication showed that evaporation is the most energy-consuming step during hydrogen production from ethanol and water [26]. Therefore, it was justified to search for a technology that would be efficient for the stoichiometric composition of the reactor feed stream.

A carbon deposit was formed on the catalyst (Figure 5), but this deposit did not cover all the cobalt. Cobalt was visible on the surface of the spent catalyst. Oxygen was also present, which may be beneficial because cobalt oxide has photocatalytic properties [37], and the spark discharge is a good source of photons [38]. Carbon was detected in the XRD analysis of the used catalyst (Figure 6). Carbon was in the form of graphite and did not form chemical compounds with cobalt.

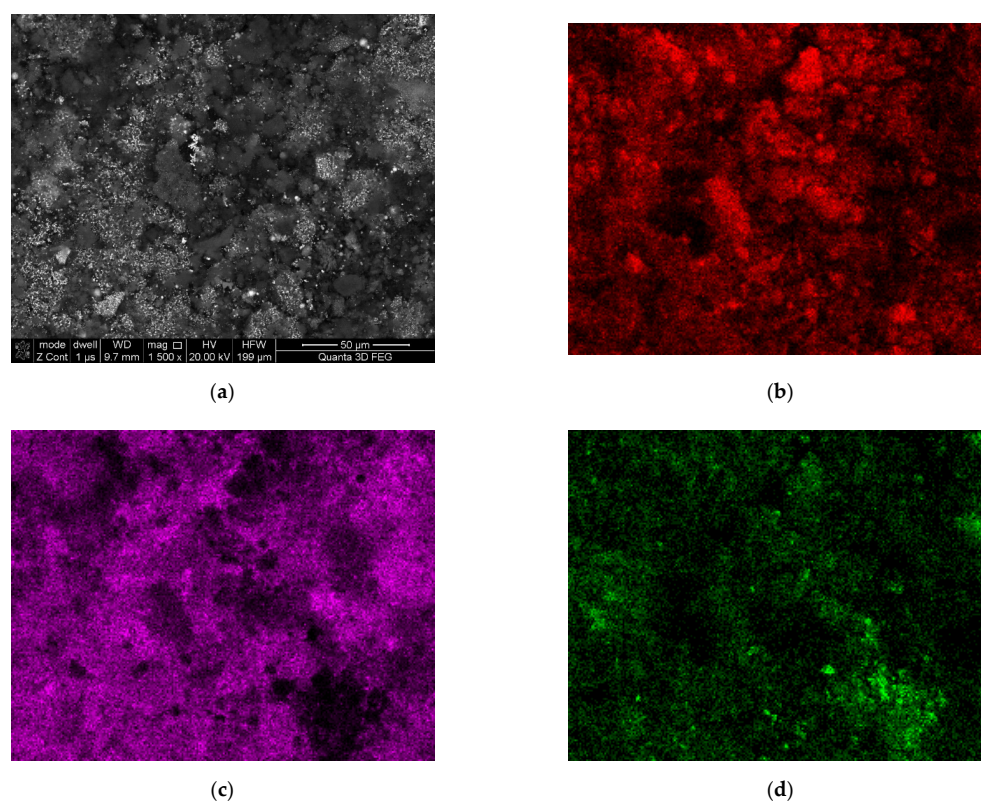


Figure 5. SEM image and EDS maps of element distributions on the surface of the used catalyst. Power—25 W. Temperature—500 °C. (a) Analyzed area. Magnification $\times 1500$; (b) carbon; (c) cobalt; (d) oxygen.

A carbon deposit may be formed in several parallel reactions in hydrogen production from ethanol. The Boudouard reaction ($2\text{CO} \rightleftharpoons \text{C} + \text{CO}_2$) and the decomposition of methane ($\text{CH}_4 \rightleftharpoons \text{C} + 2\text{H}_2$) can occur in the gas phase. However, the process conditions are unfavorable to these reactions. The exothermic Boudouard reaction ($\Delta H^\circ_{298} = -172.5 \text{ kJ/mol}$) is inhibited by high temperature, and the presence of hydrogen formed in the spark discharge inhibits the endothermic reaction of methane decomposition ($\Delta H^\circ_{298} = 74.9 \text{ kJ/mol}$). The leading cause of carbon deposition may be the presence of a C-C bond in ethanol. This bond causes ethylene and acetylene to form from ethanol. These substances polymerize easily. The polymer is then dehydrated, and carbon remains on the surface. As a result of this process, various carbon structures, e.g., encapsulating and whisker-like, are formed. A small part of the deposited carbon was whisker-like (Figure 7). It was opposite to our previous research on hydrogen production from methanol in a plasma-catalytic reactor, where mainly whisker-like carbon was formed [19]. The TPO measurement (Figure 8) shows that the primary signal was at 482 °C, and the satellite signal was at 580 °C. In the

studies devoted to analyzing carbon deposits, the signal recorded at a lower temperature was ascribed to amorphous carbon, while the signal recorded at a higher temperature corresponded to whisker-like carbon. The signal at 580 °C recorded for the studied catalyst was very small and hardly visible. A similar course was recorded by Jiang et al. [39]. A small signal indicates a small share of whisker-like carbon in the deposit. Whisker-like carbon structures are porous and gas-permeable. Therefore, their presence is preferable to the encapsulating forms. Even a small amount of whisker-like carbon allows the reagent to have access to cobalt, and the catalyst activity is high for several hours. Then, it begins to decrease slowly. As a result of the difficult access of reagents to the catalyst surface, ethanol conversion and hydrogen production decreased (Figure 9a). However, hydrogen production decreased faster than ethanol conversion. This was due to the reduced importance of the water–gas shift reaction, which also took place on the catalyst. As a result, the selectivity of ethanol conversion to carbon monoxide increased, and to carbon dioxide decreased (Figure 9b).

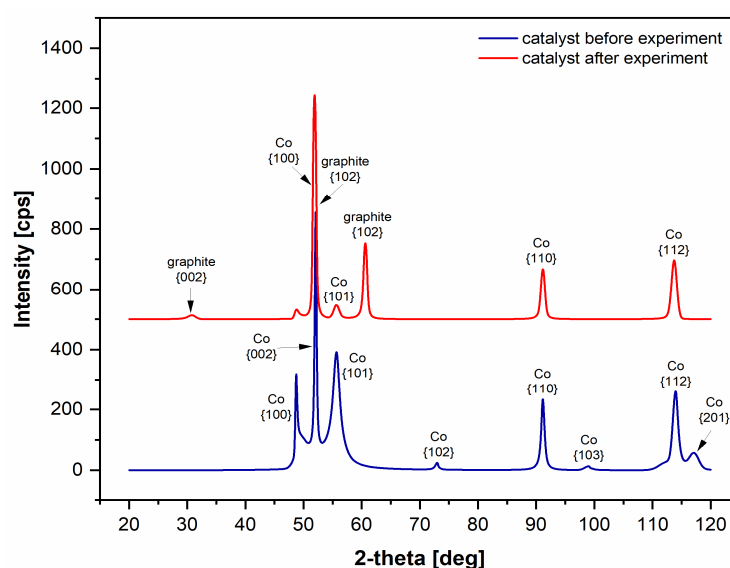


Figure 6. XRD patterns of the fresh and used catalyst.



Figure 7. SEM image of the surface of the used catalyst. Magnification $\times 50,000$. Power—25 W. Temperature—500 °C.

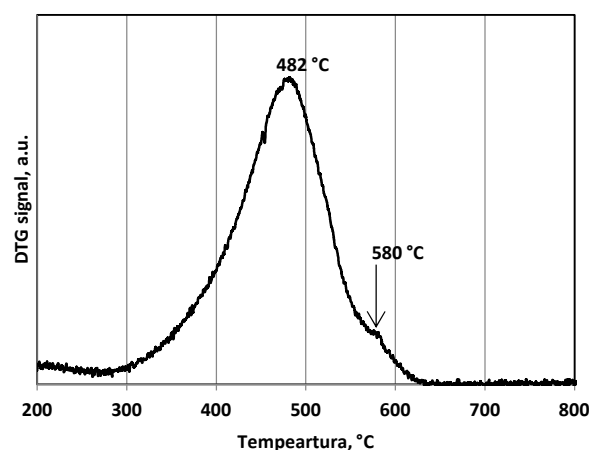
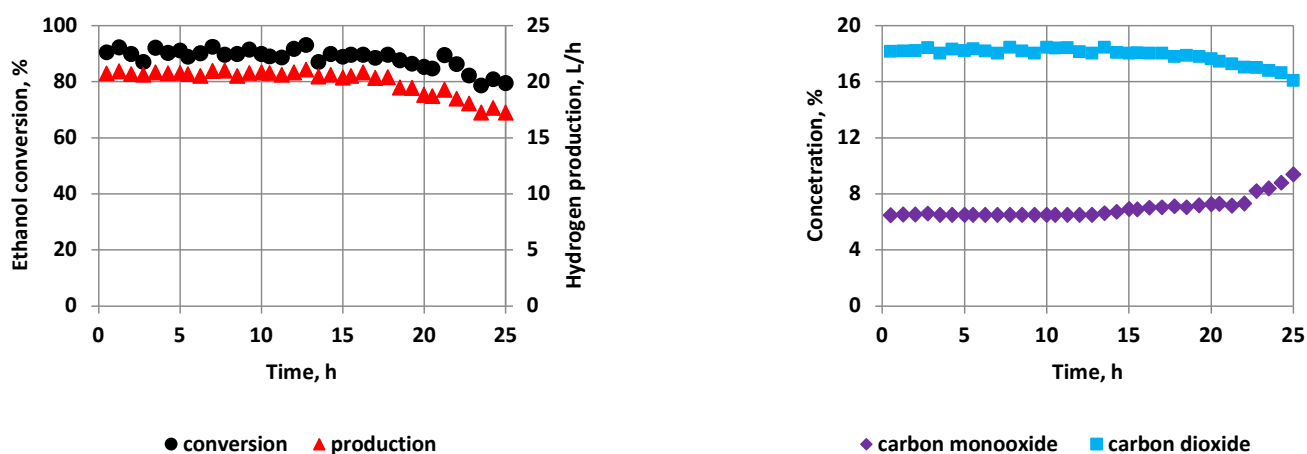


Figure 8. TPO profiles of the carbon deposited on the used catalyst. Power—25 W. Temperature—500 °C.



(a)

(b)

Figure 9. Stability performance of the catalyst. Power—25 W. Temperature—450 °C. (a) Ethanol conversion and hydrogen production; (b) CO and CO₂ concentration.

4. Conclusions

Hydrogen production from a mixture of ethanol and water in a plasma-catalytic reactor was characterized by high ethanol conversion and hydrogen production efficiency. It was observed that the catalyst was active at a temperature of 250 °C, and its activity increased with increasing temperature to 450 °C. After that, the activity remained high. The discharge power mainly influenced hydrocarbon production. Contrarily, the influence of the catalyst bed temperature on the production of hydrocarbons was minimal. On the other hand, hydrogen and CO₂ production increased with the increase in the temperature of the catalyst bed, and the production of CO decreased. It is a very positive phenomenon because it enables a high hydrogen yield using a stoichiometric molar ratio of water to ethanol.

Author Contributions: Conceptualization, B.U.; methodology, B.U., P.J., M.M. and Ł.N.; validation, B.U. and K.K.; formal analysis, B.U.; investigation, B.U., P.J., Ł.N. and M.M.; resources, B.U., P.J. and K.K.; data curation, B.U.; writing—original draft preparation, B.U.; writing—review and editing, B.U.; supervision, B.U.; funding acquisition, K.K. All authors have read and agreed to the published version of the manuscript.

Funding: This research was funded by Warsaw University of Technology.

Institutional Review Board Statement: Not applicable.

Informed Consent Statement: Not applicable.

Data Availability Statement: Not applicable.

Conflicts of Interest: The authors declare no conflict of interest. The funders had no role in the design of the study; in the collection, analyses, or interpretation of data; in the writing of the manuscript, or in the decision to publish the results.

References

1. Whitehouse Associates. *Statistical Review of World Energy 2021*, 70th ed.; Whitehouse Associates: London, UK, 2021.
2. Sarno, M.; Ponticorvo, E. High hydrogen production rate on RuS₂@MoS₂ hybrid nanocatalyst by PEM electrolysis. *Int. J. Hydrogen Energy* **2019**, *44*, 4398–4405. [\[CrossRef\]](#)
3. Nahar, G.; Mote, D.; Dupont, V. Hydrogen production from reforming of biogas: Review of technological advances and an Indian perspective. *Renew. Sustain. Energy Rev.* **2017**, *76*, 1032–1052. [\[CrossRef\]](#)
4. Lachén, J.; Herguido, J.; Peña, J.A. Production and purification of hydrogen by biogas combined reforming and steam-iron process. *Int. J. Hydrogen Energy* **2019**, *44*, 19244–19254. [\[CrossRef\]](#)
5. Tahir, M.; Mulewa, W.; Amin, N.A.S.; Zakaria, Z.Y. Thermodynamic and experimental analysis on ethanol steam reforming for hydrogen production over Ni-modified TiO₂/MMT nanoclay catalyst. *Energy Convers. Manag.* **2017**, *154*, 25–37. [\[CrossRef\]](#)
6. Mosinska, M.; Stępińska, N.; Maniukiewicz, W.; Rogowski, J.; Mierczynska-Vasilev, A.; Vasilev, K.; Szynkowska, M.I.; Mierczynski, P. Hydrogen Production on Cu-Ni Catalysts via the Oxy-Steam Reforming of Methanol. *Catalysts* **2020**, *10*, 273. [\[CrossRef\]](#)
7. Konsolakis, M.; Ioakimidis, Z.; Kraia, T.; Marnellos, G.E. Hydrogen Production by Ethanol Steam Reforming (ESR) over CeO₂ Supported Transition Metal (Fe, Co, Ni, Cu) Catalysts: Insight into the Structure-Activity Relationship. *Catalysts* **2016**, *6*, 39. [\[CrossRef\]](#)
8. Ma, Y.; Guan, G.; Shi, C.; Zhu, A.; Hao, X.; Wang, Z.; Kusakabe, K.; Abudula, A. Low-temperature steam reforming of methanol to produce hydrogen over various metal-doped molybdenum carbide catalysts. *Int. J. Hydrogen Energy* **2014**, *39*, 258–266. [\[CrossRef\]](#)
9. Tatarova, E.; Bundaleska, N.; Dias, F.M.; Tsyganov, D.; Saavedra, R.; Ferreira, C.M. Hydrogen production from alcohol reforming in a microwave 'tornado'-type plasma. *Plasma Sources Sci. Technol.* **2013**, *22*, 065001. [\[CrossRef\]](#)
10. Ulejczyk, B.; Krawczyk, K.; Młotek, M.; Nogal, Ł.; Jóźwik, P.; Bojar, Z. Steam reforming of ethanol in spark discharge generated between electrodes made from a Ni₃Al alloy. In Proceedings of the 2017 International Aegean Conference on Electrical Machines and Power Electronics (ACEMP) & 2021 International Conference on Optimization of Electrical and Electronic Equipment (OPTIM), Brasov, Romania, 25–27 May 2017; pp. 1063–1068. [\[CrossRef\]](#)
11. Ulejczyk, B.; Nogal, Ł.; Młotek, M.; Krawczyk, K. Enhanced production of hydrogen from methanol using spark discharge generated in a small portable reactor. *Energy Rep.* **2022**, *8*, 183–191. [\[CrossRef\]](#)
12. Ulejczyk, B.; Nogal, Ł.; Młotek, M.; Krawczyk, K. Efficient Plasma Technology for the Production of Green Hydrogen from Ethanol and Water. *Energies* **2022**, *15*, 2777. [\[CrossRef\]](#)
13. Burlica, R.; Shin, K.Y.; Hnatiuc, B.; Locke, B.R. Hydrogen generation by pulsed gliding arc discharge plasma with sprays of alcohol solutions. *Ind. Eng. Chem. Res.* **2011**, *50*, 9466–9470. [\[CrossRef\]](#)
14. Ulejczyk, B.; Nogal, Ł.; Młotek, M.; Krawczyk, K. Hydrogen production from ethanol using dielectric barrier discharge. *Energy* **2019**, *174*, 261–268. [\[CrossRef\]](#)
15. Du, C.; Ma, D.; Wu, J.; Lin, Y.; Xiao, W.; Ruan, J.; Huang, D. Plasma-catalysis reforming for H₂ production from ethanol. *Int. J. Hydrogen Energy* **2015**, *40*, 15398–15410. [\[CrossRef\]](#)
16. Ulejczyk, B.; Nogal, Ł.; Młotek, M.; Falkowski, P.; Krawczyk, K. Hydrogen production from ethanol using a special multi-segment plasma-catalytic reactor. *J. Energy Inst.* **2021**, *95*, 179–186. [\[CrossRef\]](#)
17. Li, X.S.; Wang, L.Y.; Gong, X.L.; Lian, H.L.; Liu, J.L.; Zhu, A.M. Evaluation of plasma-derived heat and synergistic effect for in-plasma catalytic steam reforming of methanol. *J. Phys. D Appl. Phys.* **2020**, *53*, 104003. [\[CrossRef\]](#)
18. Zhu, X.; Hoang, T.; Lobban, L.L.; Mallinson, R.G. Low CO content hydrogen production from bio-ethanol using a combined plasma reforming-catalytic water gas shift reactor. *Appl. Catal. B Environ.* **2010**, *94*, 311–317. [\[CrossRef\]](#)
19. Ulejczyk, B.; Nogal, Ł.; Jóźwik, P.; Młotek, M.; Krawczyk, K. Plasma-Catalytic Process of Hydrogen Production from Mixture of Methanol and Water. *Catalysts* **2021**, *11*, 864. [\[CrossRef\]](#)
20. Khoja, A.H.; Azad, A.K.; Saleem, F.; Khan, B.A.; Naqvi, S.R.; Mehran, M.T.; Amin, N.A.S. Hydrogen Production from Methane Cracking in Dielectric Barrier Discharge Catalytic Plasma Reactor Using a Nanocatalyst. *Energies* **2020**, *13*, 5921. [\[CrossRef\]](#)
21. Mei, D.; Ashford, B.; He, Y.L.; Tu, X. Plasma-catalytic reforming of biogas over supported Ni catalysts in a dielectric barrier discharge reactor: Effect of catalyst supports. *Plasma Process. Polym.* **2017**, *14*, e1600076. [\[CrossRef\]](#)
22. Zhu, F.S.; Zhang, H.; Yan, X.; Yan, J.H.; Ni, M.J.; Li, X.D.; Tu, X. Plasma-catalytic reforming of CO₂-rich biogas over Ni/ γ -Al₂O₃ catalysts in a rotating gliding arc reactor. *Fuel* **2017**, *199*, 430–437. [\[CrossRef\]](#)
23. Ulejczyk, B.; Nogal, Ł.; Jóźwik, P.; Młotek, M.; Krawczyk, K. A Promising Cobalt Catalyst for Hydrogen Production. *Catalysts* **2022**, *12*, 278. [\[CrossRef\]](#)
24. Mhadmhan, S.; Natewong, P.; Prasongthum, N.; Samart, C.; Reubroycharoen, P. Investigation of Ni/SiO₂ Fiber Catalysts Prepared by Different Methods on Hydrogen production from Ethanol Steam Reforming. *Catalysts* **2018**, *8*, 319. [\[CrossRef\]](#)
25. Greluk, M.; Rotko, M.; Turczyniak-Surdacka, S. Enhanced catalytic performance of La₂O₃ promoted Co/CeO₂ and Ni/CeO₂ catalysts for effective hydrogen production by ethanol steam reforming. *Renew. Energy* **2020**, *155*, 378–395. [\[CrossRef\]](#)

26. Ulejczyk, B.; Nogal, Ł.; Józwiak, P.; Młotek, M.; Krawczyk, K. Hydrogen production from ethanol in dielectric barrier discharge. In Proceedings of the 2021 International Aegean Conference on Electrical Machines and Power Electronics (ACEMP) & 2021 International Conference on Optimization of Electrical and Electronic Equipment (OPTIM), Brasov, Romania, 2–3 September 2021; pp. 358–363. [[CrossRef](#)]
27. La Civita, G.; Orlandi, F.; Mariani, V.; Cazzoli, G.; Ghedini, E. Numerical Characterization of Corona Spark Plugs and Its Effects on Radicals Production. *Energies* **2021**, *14*, 381. [[CrossRef](#)]
28. Overand, R.; Paraskevopoulos, G. Rates of hydroxyl radical reactions. 4. Reactions with methanol, ethanol, 1-propanol, and 2-propanol at 296 K. *J. Phys. Chem.* **1998**, *82*, 1329–1333. [[CrossRef](#)]
29. Owens, C.; Roscoe, J. The reactions of atomic oxygen with methanol and ethanol. *Can. J. Chem.* **2011**, *54*, 984–989. [[CrossRef](#)]
30. Baraj, E.; Ciahotný, K.; Hlinčík, T. Advanced Catalysts for the Water Gas Shift Reaction. *Crystals* **2022**, *12*, 509. [[CrossRef](#)]
31. Baránková, H.; Bardos, L.; Bardos, A. on-conventional atmospheric pressure plasma sources for production of hydrogen. *MRS Adv.* **2018**, *3*, 921–929. [[CrossRef](#)]
32. Bardos, L.; Barankova, H.; Bardos, A. Production of hydrogen-rich synthesis gas by pulsed atmospheric plasma submerged in mixture of water with ethanol. *Plasma Chem. Plasma Process.* **2017**, *37*, 115–123. [[CrossRef](#)]
33. Zhu, T.; Sun, B.; Zhu, X.; Wang, L.; Xin, Y.; Liu, J. Mechanism analysis of hydrogen production by microwave discharge in ethanol liquid. *J. Anal. Appl. Pyrolysis* **2021**, *156*, 105111. [[CrossRef](#)]
34. Xin, Y.; Sun, B.; Zhu, X.; Yan, Z.; Sun, X. Hydrogen-rich syngas production by liquid phase pulsed electrodeless discharge. *Energy* **2021**, *214*, 118902. [[CrossRef](#)]
35. Tsymbalyuk, A.N.; Levko, D.S.; Chernyak, V.Y.; Martysh, E.V.; Nedybalyuk, O.A.; Solomenko, E.V. Influence of the Gas Mixture Temperature on the Efficiency of Synthesis Gas Production from Ethanol in a Nonequilibrium Plasma. *Tech. Phys.* **2013**, *58*, 1138–1143. [[CrossRef](#)]
36. Chernyak, V.Y.; Olszewski, S.V.; Yukhymenko, V.V.; Solomenko, E.V.; Prysiazhnevych, I.V.; Naumov, V.V.; Levko, D.S.; Shchedrin, A.I.; Ryabtsev, A.V.; Demchina, V.P.; et al. Plasma-Assisted Reforming of Ethanol in Dynamic Plasma-Liquid System: Experiments and Modeling. *IEEE Trans. Plasma Sci.* **2008**, *36*, 2933–2939. [[CrossRef](#)]
37. Moridon, S.N.F.; Salehmin, M.I.; Mohamed, M.A.; Arifin, K.; Minggu, L.J.; Kassim, M.B. Cobalt oxide as photocatalyst for water splitting: Temperature-dependent phase structures. *Int. J. Hydrogen Energy* **2019**, *44*, 25495–25504. [[CrossRef](#)]
38. Piskarev, I.M.; Ivanova, I.P.; Trofimova, S.V.; Aristova, N.A. Formation of active species in spark discharge and their possible use. *High Energy Chem.* **2012**, *46*, 343–348. [[CrossRef](#)]
39. Jiang, Z.; Liao, X.; Zhao, Y. Comparative study of the dry reforming of methane on fluidized aerogel and xerogel Ni/Al₂O₃ catalysts. *Appl. Petrochem. Res.* **2013**, *3*, 91–99. [[CrossRef](#)]